Economic Geology
Vol. 97, 2002, pp. 1063–1077

A8

Genesis of the Doğankuzu and Mortaş Bauxite Deposits, Taurides, Turkey: Separation of Al, Fe, and Mn and Implications for Passive Margin Metallogeny

Hüseyin Öztürk,†
Geology Department, Istanbul University, Avcılar, 34850, Istanbul, Turkey

James R. Hein,
U.S. Geological Survey, MS 999, 345 Middlefield Road, Menlo Park, California 94025

and Nurullah Hanilçi
Geology Department, Istanbul University, Avcılar, 34850, Istanbul, Turkey

Abstract

The Taurides region of Turkey is host to a number of important bauxite, Al-rich laterite, and Mn deposits. The most important bauxite deposits, Doğankuzu and Mortaş, are karst-related, unconformity-type deposits in Upper Cretaceous limestone. The bottom contact of the bauxite ore is undulatory, and bauxite fills depressions and sinkholes in the footwall limestone, whereas its top surface is concordant with the hanging-wall limestone. The thickness of the bauxite varies from 1 to 40 m and consists of böhmite, hematite, pyrite, marcasite, anatase, diaspore, gypsum, kaolinite, and smectite. The strata-bound, sulfide- and sulfate-bearing, low-grade lower part of the bauxite ore bed contains pyrite pseudomorphs after hematite and is deep red in outcrop owing to supergene oxidation. The lower part of the bauxite body contains local intercalations of calcareous conglomerate that formed in fault-controlled depressions and sinkholes. Bauxite ore is overlain by fine-grained Fe sulfide-bearing and calcareous claystone and argillaceous limestone, which are in turn overlain by massive, compact limestone of Santonian age. That 50-m-thick limestone is in turn overlain by well-bedded bioclastic limestone of Campanian or Maastrichtian age, rich with rudist fossils. Fracture fillings in the bauxite orebody are up to 1 m thick and consist of bluish-gray-green pyrite and marcasite (20%) with böhmite, diaspore, and anatase. These sulfide veins crosscut and offset the strata-bound sulfide zones. Sulfur for the sulfides was derived from the bacterial reduction of seawater sulfate, and Fe was derived from alteration of oxides in the bauxite. Iron sulfides do not occur within either the immediately underlying or overlying limestone.

The platform limestone and shale that host the bauxite deposits formed at a passive margin of the Tethys Ocean. Extensive vegetation developed on land as the result of a humid climate, thereby creating thick and acidic soils and enhancing the transport of large amounts of organic matter to the ocean. Alteration of the organic matter provided CO_2 that contributed to formation of a relatively ^{12}C-rich marine footwall limestone. Relative sea-level fall resulted from strike-slip faulting associated with closure of the ocean and local uplift of the passive margin. That uplift resulted in karstification and bauxite formation in topographic lows, as represented by the Doğankuzu and Mortaş deposits. During stage 1 of bauxite formation, Al, Fe, Mn, and Ti were mobilized from deeply weathered aluminosilicate parent rock under acidic conditions and accumulated as hydroxides at the limestone surface owing to an increase in pH. During stage 2, Al, Fe, and Ti oxides and clays from the incipient bauxite (bauxitic soil) were transported as detrital phases and accumulated in the fault-controlled depressions and sinkholes. During stage 3, the bauxitic material was concentrated by repeated desilicification, which resulted in the transport of Si and Mn to the ocean through a well-developed karst drainage system. The transported Mn was deposited in offshore muds as Mn carbonates. The sulfides also formed in stage 3 during early diagenesis. Transgression into the foreland basin resulted from shortening of the ocean basin and nappe emplacement during the latest Cretaceous. During that time bioclastic limestone was deposited on the nappe ramp, which overlapped bauxite accumulation.

Introduction

The formation of large Al, Fe, and Mn deposits at passive margins, and particularly the processes responsible for the separation of Al from the other metal oxides into different deposit types, are not well understood (Hem, 1972; Hutchinson, 1983; Sawkins, 1984; Ostwald and Bolton, 1992; Glasby, 1997). A large variety of these deposit types occurs in the same metallogenic province in passive-margin deposits of the Taurides region of southern Turkey, including karst-related bauxite deposits (Özlü, 1978), Al-rich laterite deposits and Fe-rich bauxites (Ayhan and Karadağ, 1985), Mn deposits (Öztürk and Hein, 1997) (Fig. 1A), and carbonate-hosted Pb-Zn deposits (Çevrim, 1984). The Mn deposits formed in deep to middle-depth marine environments near the time of the Cenomanian-Turonian transition (Öztürk and Hein, 1997), whereas coeval bauxite and Fe-rich bauxite deposits formed in an adjacent terrestrial environment.

Established models of karst-related, unconformity-type bauxite deposits generally emphasize in situ alteration and production of residual material from the leaching of either the limestone or associated pyroclastic debris, which forms a blanket of bauxitic material on a limestone karst surface (e.g., Bárdossy, 1982; D'Argenio and Mindszenty, 1995). The deposit structure and the geometry of the karst surface can

† Corresponding author: e-mail, ozturkh@istanbul.edu.tr

0361-0128/01/3273/1061-15 $6.00

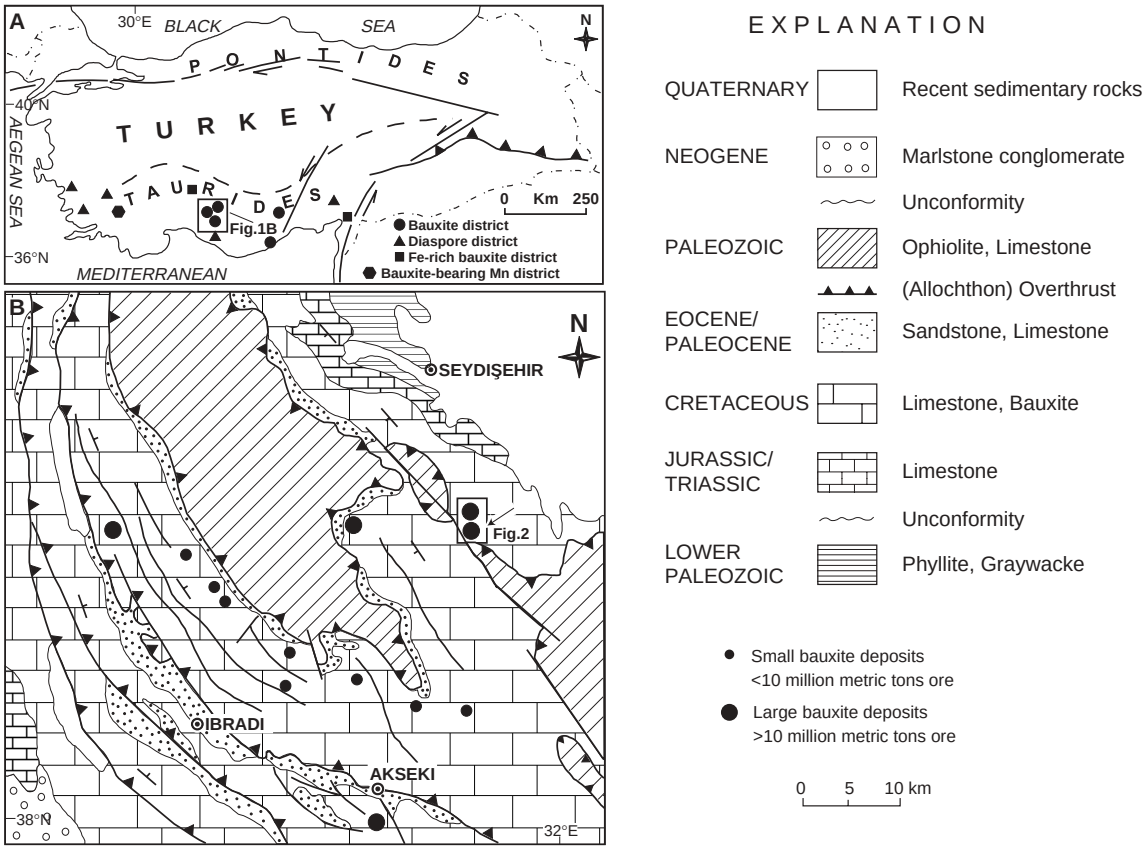

FIG. 1. A. Map showing major Al and Mn deposits of the Taurides region. B. Geologic map of the Seydişehir-Akseki bauxite province (modified from Monod, 1977).

define a wide variety of subtypes of karst-related bauxite deposits. The bauxitic material may remain in place where the parent rock was leached, common in deep sinkholes in high-elevation terrain, or it may be transported to karst depressions, common in low-elevation terrain (e.g., Valeton et al., 1987; D'Argenio and Mindszenty, 1995).

In this paper, the bauxite deposits of the Seydişehir region (Mortaş and Doğankuzu deposits) are examined in terms of field relations, lithologic associations, petrography, mineralogy, and chemistry, and carbon, oxygen, and sulfur isotopes. The objectives were to determine the deposit characteristics, the terrestrial paleoenvironmental conditions in the region where Fe-rich bauxite formed from Cenomanian through Santonian, and the processes responsible for the mobilization, fractionation, and deposition of Al, Fe, and Mn during that time. On the basis of these observations, we propose a model for passive-margin metallogeny for metal-oxide deposits of southern Turkey.

Geologic Setting

The region studied is located in the central Taurides Mountains, where the geologic framework comprises major autochthonous and allochthonous tectonostratigraphic units. The autochthonous unit consists of lower Paleozoic phyllite and graywacke known as the Seydişehir schist. Triassic and Jurassic limestone and dolomitic limestone unconformably overlie the Paleozoic strata. Cretaceous rocks include more than 1,000 m of carbonates consisting of limestone, dolomitic limestone, and associated bauxites. Paleocene and Eocene limestone and sandstone conformably overlie Cretaceous rocks (Fig. 1B). The allochthonous unit consists of two tectonostratigraphic subunits: serpentinized ultramafic-mafic rocks and limestone and dolostone of Permian age, known as the Hadım nappes (Monod, 1977). During the Oligocene, allochthonous units were probably obducted from the north onto the autochthonous basement. Posttectonic sedimentary rocks consist of alluvial fan deposits of Miocene and Pliocene ages.

Bauxite Deposits

The most economically important bauxite deposits of Turkey occur in the Seydişehir-Akseki region of the central Taurides Mountains (Blumental and Göksu, 1949; Göksu, 1953; Wippern, 1962; Özlü, 1978, 1979; Patterson et al., 1986; Karadağ, 1987; Öztürk et al., 1998; Bárdossy and Combes, 1999). The Mortaş and Doğankuzu deposits, which are karst unconformity-type deposits, are the most important deposits in that region and are mined by the Seydişehir aluminum company. Large open pits allow detailed field observations of contact relations and lateral and vertical changes in ore structure and ore types. The deposits occur at the crest of the Taurides Mountains between 1,500 and 2,000 m above sea level. Bauxite formed at an unconformity surface that is nearly concordant with the host platform limestone of

Cretaceous age. The north-south–trending and gently dipping bauxite bed is cut by normal faults with nearly 1 km of offset (Fig. 2). The ore thickness varies from 1 to 40 m.

Detailed exploration (50 m grid over 1.2 km^2) of the Mortaş bauxite deposit from 1970 to 1980 determined that there was 10.9 million metric tons of ore at 57 percent Al_2O_3. Six million metric tons of ore was produced through 1998 leaving about 5 million tons of ore reserves. The Doğankuzu bauxite deposit is located 2 km southwest of the Mortaş deposit and has 14.9 million metric tons of ore at 58 percent Al_2O_3 (A. Pelen, unpublished Etibank reports, 1973, 1977; A. Pelen and A. Vuran, unpublished Etibank report, 1978). Lower-grade Fe sulfide-rich ore has a grade of 45 percent Al_2O_3 and is 1 to 2 m thick. Three million tons of ore have been mined from the deposit through 1998. Annual production from the Doğankuzu deposit is 300,000 metric tons; the ore is transported to the Seydişehir aluminum factory where 60,000 tons of aluminum metal are extracted.

The Mortaş deposit

The Mortaş bauxite deposit is located on the southeastern slope of Mortaş Hill. The deposit is 400 m long and up to 40 m thick; it averages 10 m thick (Fig. 3). The ore is truncated by faults, and horizontal offsets of the ore bed can be more than 200 m. The well-bedded footwall limestone is massive with extensive karst development below the unconformity, including well-developed sinkholes and duden structures (covered or hidden sinks for surface drainage). The base of the orebody contains undulations where bauxite filled depressions and paleosinkholes in the footwall limestone. The upper contact of the bauxite is concordant with hanging-wall limestone. In places the footwall limestone is brecciated and cemented by Al hydroxides.

The lower part of the bauxite bed contains Fe sulfide-rich, grayish-green, low-grade ore that grades laterally into Fe oxide-rich, pinkish-brown bauxite. The low-grade ore, composed of böhmite, hematite, diaspore, calcite, and pyrite, is overlain by dark-brown, pisolitic, conglomerate ore. The pisolitic ore is concordant with both footwall and hanging-wall limestones. Pisolites (banded, >2 mm diameter) range up to 1 cm in diameter and are composed chiefly of hematite; the pisolitic ore grades into relatively high-grade massive ore. Bauxite is composed of böhmite, hematite, goethite, diaspore, and anatase. X-ray–amorphous alumogels were also reported in the ores (Atabey, 1976).

Iron sulfide-bearing veins and disseminated Fe sulfides are especially common in the lower and upper parts of the bauxite bed. The grayish-blue, Fe sulfide-rich zone that occurs in the lower part of the bauxite bed is earthy and is noted in the quarry for its unpleasant odor; this horizon is referred to as

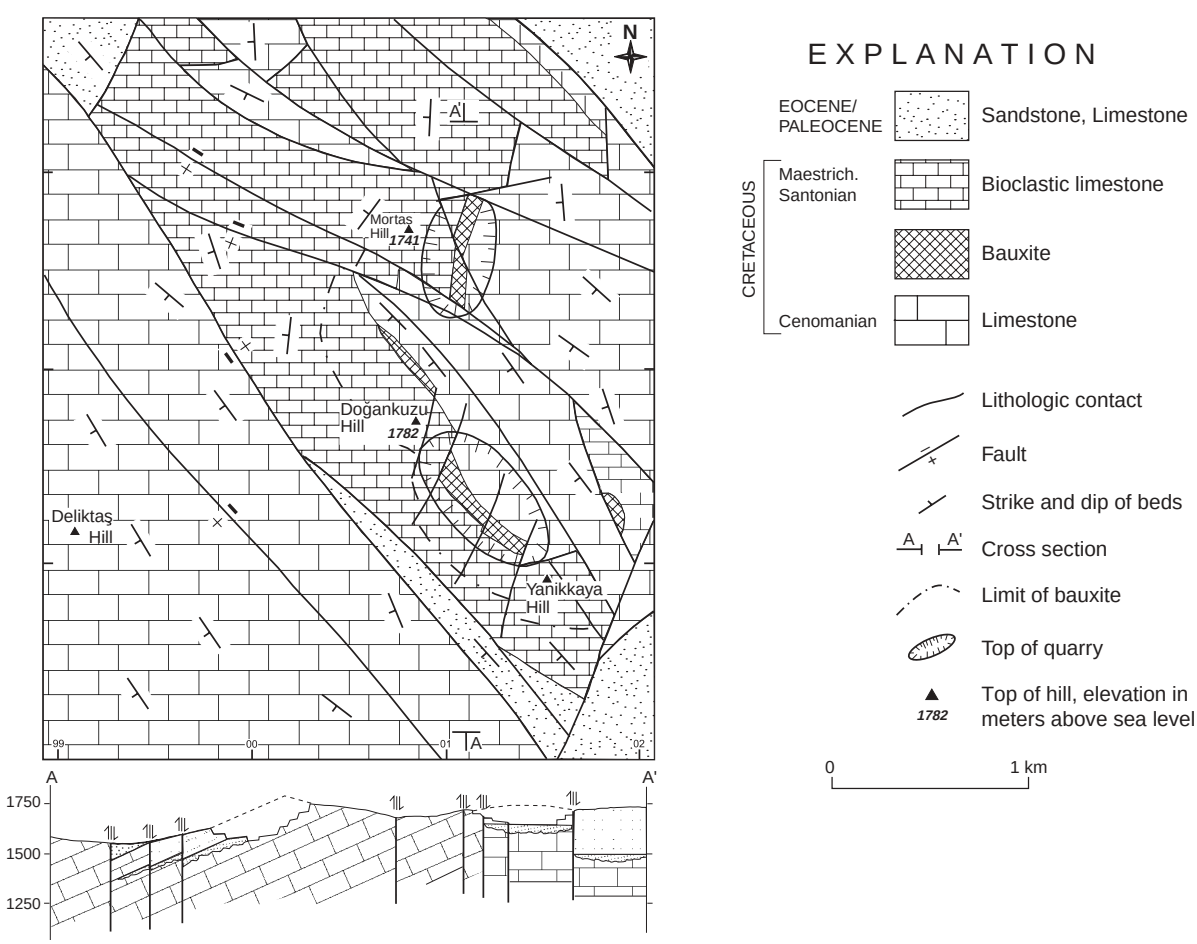

FIG. 2. Geologic map and cross section of the Mortaş and Doğankuzu bauxite district.

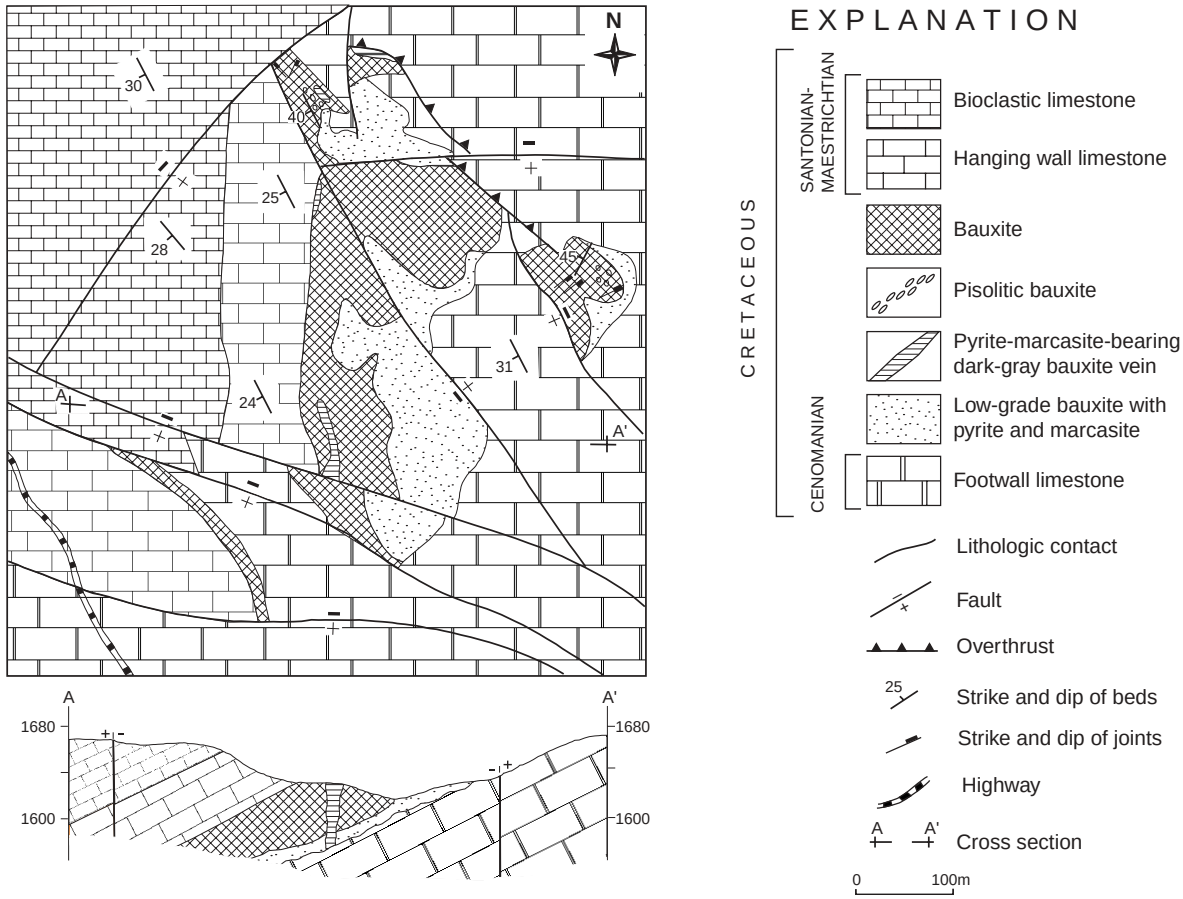

FIG. 3. Geologic map and cross section of the Mortaş bauxite deposit.

the bottom sulfide zone. The bauxite bed is overlain by disseminated pyrite- and marcasite-bearing argillaceous limestone, which is overlain by pale-brown siliceous limestone. Iron oxides in the uppermost part of the bauxite bed are derived from oxidation of sulfides; this horizon and the overlying sulfides in the argillaceous limestone are referred to as the top sulfide zone. Low-grade, Fe sulfide-rich veins 1 to 3 m thick crosscut the bauxite.

The Doğankuzu bauxite deposit

The Doğankuzu bauxite deposit shows excellent relations between the bauxite and the footwall and hanging-wall limestones. This deposit was sampled for chemical and stable isotope analyses. Host-rock characteristics are comparable to those of the Mortaş deposit (Fig. 4). The base of the bauxite is undulatory, whereas the top contact is concordant with the overlying limestone. The footwall limestone forms a monotonous 1-km-thick succession that has been dated as Cenomanian (A. Pelen, unpublished Etibank report, 1973; Özlü, 1978) or Early Cretaceous age (Blumental and Göksu, 1949). Locally, strata adjacent to the ore are brecciated and cemented by bauxite.

The lower ore section begins with grayish-green, dark-gray, earthy, Fe sulfide-rich, low-grade ore. This ore horizon shows pseudo-oolitic texture (faint or no internal banding of ooids), and pseudo-ooids are visible to the naked eye. Locally, oxidation of this horizon has produced pale-brown, skeletal, Fe-rich bauxite ore. This deposit does not include pisolitic ore.

In places, the lower bauxite ore section is intercalated with up to three calcareous conglomerate lenses (Fig. 5). Textural evidence indicates that these conglomerates were deposited by mass-flow gravity processes. Limestone clasts in the conglomerate are generally 3 to 5 cm in diameter but range up to 30 cm. The conglomerate lenses average 0.3 m thick and extend up to 30 m in length. The bauxite, which accumulated coevally in the same fault-controlled depressions in the limestone, forms the matrix of the conglomerates. Güldalı (1973) suggested that the bauxites are paleosinkhole deposits because of their delta-shaped geometry in cross section. Some of the filled depressions clearly did originate as sinkholes, but the predominant control on karst structures was faulting.

High-grade ore is overlain by a 5- to 10-cm-thick, yellowish pale-brown, very fine grained pyrite-bearing limestone. Hanging-wall limestone is massive, up to 50 m thick, pale-brown to white, and compact. This limestone was previously dated as Late Cretaceous, either Turonian (A. Pelen, unpublished Etibank report, 1973; Özlü, 1978) or Santonian (Blumental and Göksu, 1949). We determined the age of limestone samples C-7 and C-8, on the basis of *Murciella* sp., *Nazzazeta* sp., *Minouxia* sp., *Minouixa conica* Gedrot, *Montcharmontxia apeminica*, *Discorbis* sp., and *Radshoovenia cf. salentina* fossils, to be clearly of Santonian age. Thus,

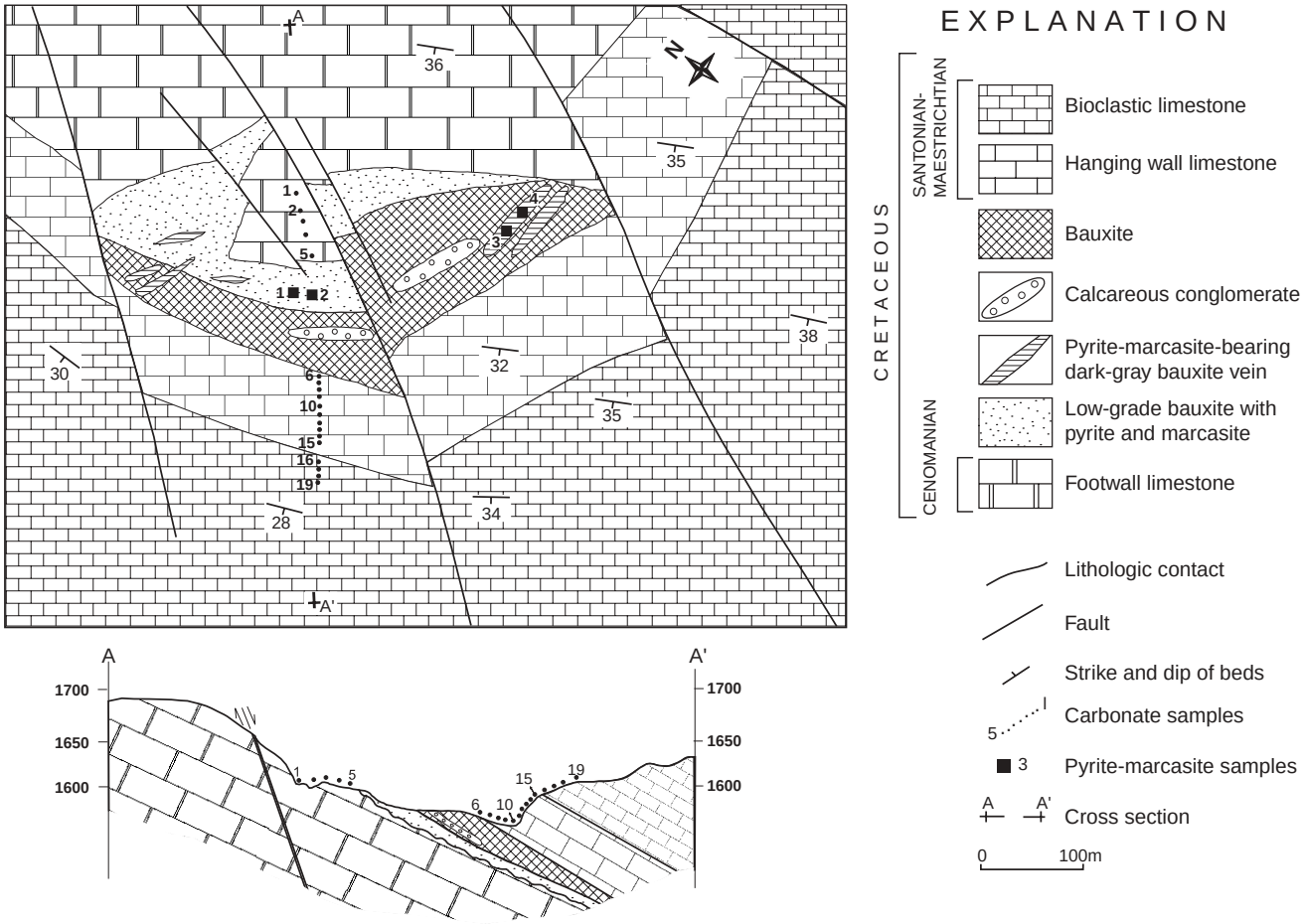

FIG. 4. Geologic map and cross section of the Doğankuzu bauxite deposit. Note location of four sulfide samples (solid squares) listed as S-1 through S-4 in Tables 1 and 4 and of 19 carbonate samples (small dots) listed as C-1 through C-19 in Tables 1 and 3.

the bauxite formed mainly during the Turonian. Fifty meters of bluish-gray limestone occur above the hanging-wall limestone. This unit is regionally extensive and a key stratigraphic interval containing large numbers of mostly reworked or transported rudist and gastropod macrofossils; it is characterized by white dolostone and grayish limestone intercalations. These Campanian or Maastrichtian bioclastic deposits probably formed in response to tectonic activity.

Methods

The mineralogy of the ores was studied by thin section and polished section petrography (24 samples), X-ray diffraction (28 samples), and electron microprobe (6 samples). X-ray diffraction was carried out using a Philips diffractometer with Cu kα radiation, a graphite monochromator, 40 kV, 30 mA, at 10 counts/s over a 2θ range of 4° to 70°. Microprobe analyses were completed using a computer-automated Jeol 733 electron microprobe, with a 200 s counting time, generally a 15 μm beam width, 47.6 nA beam current, and 20 kV. Although the deposits analyzed are generally fine grained, the microprobe data were obtained only on discrete single grains.

Stable isotope studies were carried out on 23 samples from Doğankuzu. Carbon and oxygen isotopes of carbonate samples were determined on CO_2 evolved from reacting samples with phosphoric acid at 90°C. Stable isotope ratios were determined using a Micromass dual inlet prism at Geochron Laboratories. For the few limestone samples that contain dolomite as well as calcite, the bulk sample was analyzed. Sulfur isotopes were determined at Geochron Laboratories on whole-rock samples in which the only detectable form of sulfur was Fe sulfide. Data were normalized to CDT with $^{34}S/^{32}S$ of 0.0450045.

Sample numbers preceded by C represent carbonate samples, by S represent sulfide-rich bauxite samples, and by B represent bauxite samples.

Analytical Results

Mineralogy and petrography

X-ray diffraction results show that the ore at Doğankuzu is predominantly böhmite and hematite, with minor anatase and smectite (Table 1). Where mineralized by sulfides, the ore also contains pyrite, marcasite, and in places diaspore, with minor kaolinite, anatase, and in some samples goethite. Hematite occurs as anhedral patches and as pseudomorphs after pyrite in the high-grade ore. Isomorphous substitution

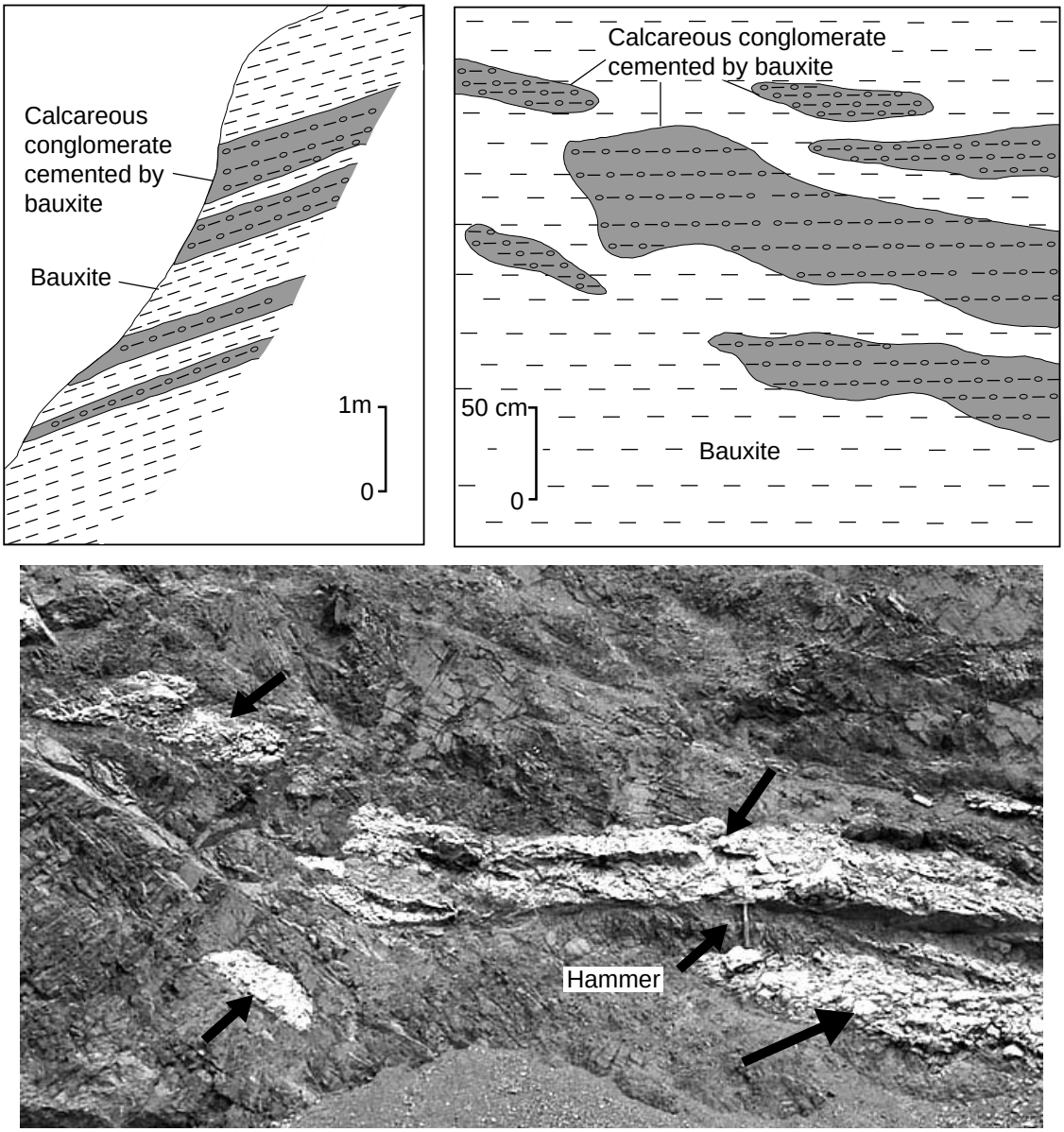

FIG. 5. Schematic and outcrop illustrations of types of intercalation of calcareous conglomerate, indicated by arrows in photograph, and bauxite at the Doğankuzu bauxite deposit; the conglomerate consists of limestone clasts in a bauxite matrix.

of Fe in böhmite was determined by microprobe to be $Al_{0.8}Fe_{0.2}O(OH)$. Comparable mineral chemistry for ferruginous böhmite has been found both experimentally and from other bauxite deposits (Cailére and Pobeguin, 1961; Franz, 1978; Bárdossy, 1982; Tardy and Nahon, 1985). White, silky kaolinite infills well-developed joints that occur at 5- to 10-cm intervals in the bauxite.

Textural analysis of the bauxite indicates that it has been reworked. For example, pisolites of various shapes and sizes, broken pisolites, and rock fragments of hematite and böhmite indicate high-energy, mass-flow depositional conditions. In contrast, hematite-sulfide replacement relations indicate that the sulfides likely formed during multiple stages at the time of böhmite-hematite deposition or, more likely, during diagenesis in response to fluctuating redox conditions.

The Fe sulfide-rich zone in the lower part of the bauxite bed locally contains pisolites with a banded structure (Fig. 6A). This texture may represent fluctuating redox conditions in depositional or diagenetic environments. The pseudo-oolitic ferruginous böhmite and nearly stoichiometric böhmite ooids (banded, ≤2 mm in diameter) occur together in some reworked bauxite clasts within the fine-grained matrix (Fig. 6B), indicating reworking and transportation of the various types of böhmite and then final accumulation of bauxitic material in the depressions.

Pisolitic bauxites consist of colloform hematite and böhmite pisolites and ooids of widely variable sizes. Colloidal deposition of Al and Fe is indicated by globular oolites and pisolites, size variability, and interposed lobe structures on the oolites. The colloform texture of hematite is especially characterized

TABLE 1. Mineralogy of Bauxite and Host Limestone as Determined by X-Ray Diffraction, Doğankuzu Deposit, Turkey

	Mineral abundance		
Sample	Major (>25%)	Moderate (5–25%)	Minor (<5%)
C-19	Calcite	Dolomite	Pyrite
C-18	Calcite	Dolomite	—
C-17	Calcite	—	Dolomite, pyrite
C-16	Calcite, dolomite	—	Pyrite, smectite
C-15	Calcite	—	Smectite, böhmite?
C-14	Calcite	—	Böhmite?
C-13	Calcite	—	Böhmite?
C-12	Calcite	—	Smectite, böhmite?
C-11	Calcite	—	Talc?
C-10	Calcite	—	Böhmite?
C-9	Calcite	—	—
C-8	Calcite	—	—
C-7	Calcite	—	Smectite, böhmite?
C-6	Calcite	—	—
B-5	Böhmite, hematite	—	Anatase, smectite
B-4	Böhmite, hematite	—	Anatase, smectite
B-3	Böhmite, hematite	—	Anatase, smectite
B-2	Böhmite, hematite	—	Anatase, smectite
B-1	Böhmite, hematite	—	Anatase, smectite
S-4	Böhmite	Pyrite	Anatase, kaolinite
S-3	Böhmite, pyrite	—	Anatase, kaolinite, goethite, marcasite?
S-2	Böhmite, pyrite	—	Marcasite, kaolinite, anatase
S-1	Böhmite, diaspore	Pyrite, marcasite	Kaolinite, anatase
C-5	Calcite	—	Böhmite?
C-4	Calcite	—	Böhmite?
C-3	Calcite	—	Böhmite?
C-2	Calcite	—	Gibbsite?
C-1	Calcite	—	Smectite

Samples are listed in stratigraphic order; S-3 and S-4 are veins in the bauxite

by pseudo-ooid development associated with interposed lobes and dehydration cracks (Fig. 6C). The high-grade ore consists of a böhmite groundmass with disseminated and colloform hematite grains (Fig. 6D).

Iron sulfides in the bauxite

Two types of sulfide deposit are associated with the bauxite (Öztürk et al., 1998). The first type is widespread and strata bound, and it occurs in the lower and upper parts of the bauxite bed; the second type is in veins. The major sulfide veins and strata-bound layers are depicted in Figures 3 and 4; however, most are too thin to be shown on the geologic maps. Early workers (A. Pelen, unpublished Etibank report, 1977; Özlü, 1978) described strata-bound sulfide occurrences but not the vein-type deposits, because of advanced surface oxidation. The Fe sulfide-rich veins grade into limonitic veins at the top of the bauxite-ore bed. They crosscut and offset the strata-bound sulfide but do not extend into the overlying or underlying host limestones. These sulfide associations vary on a district-wide scale. For example, sulfides occur in the upper part of the bauxite ore at the Arvana and Değirmenlik deposits (Özlü, 1978), but neither vein-type nor lower ore-bed sulfide deposits have been identified in those deposits.

At Doğankuzu, iron sulfide deposits in the lower part of the bauxite bed are thicker and more extensive than in the upper part of the ore bed. This bottom zone of strata-bound deposit is a distinctive grayish-blue to greenish-blue in the open pit and ranges from 1 to 10 m thick. This sulfide-rich, low-grade bauxite ore horizon locally shows a pseudo-oolitic texture cemented by sulfides. Rock from this zone is harder and yields an excellent polish compared with other sulfide-bearing samples. Aluminum contents of this interval are relatively low, and consequently it is not mined. The top Fe sulfide-rich zone is about 10 cm thick and is composed of disseminated, fine-grained pyrite and marcasite.

Dark-gray to greenish-gray vein-type Fe sulfides in the bauxite developed as fracture fillings along faults, indicating that vein mineralization was structurally controlled. The veins are discordant to the strata-bound bauxite as shown in the geologic cross section (Fig. 3). The veins are composed of böhmite, diaspore, marcasite, pyrite, and anatase, and they have a higher diaspore content than the bauxite ores. At Mortaş, veins are generally 0.4 to 2 m thick and grade up-section to yellowish-red oxidized sulfides (Fig. 7). These veins continue for up to 100 m in strike without significant change in thickness.

Minerals composing the bottom and top sulfide-rich deposits at Doğankuzu and Mortaş are similar. They consist of böhmite, diaspore, pyrite, marcasite, and anatase, local gypsum and kaolinite, and minor smectite and calcite. Locally, ooids and laminae in the bottom sulfide zone are banded by alternating böhmite and marcasite-pyrite (Fig. 8A, B). Some ooid nuclei consist of cubic pyrite. Framboidal pyrite and marcasite were not found in the sulfide-rich deposits. Typical pyrite-hematite associations include pyrite altered to hematite along crystallographic planes (Fig. 8C), hematite laths in a pyrite matrix (Fig. 8D), and pyrite pseudomorphs

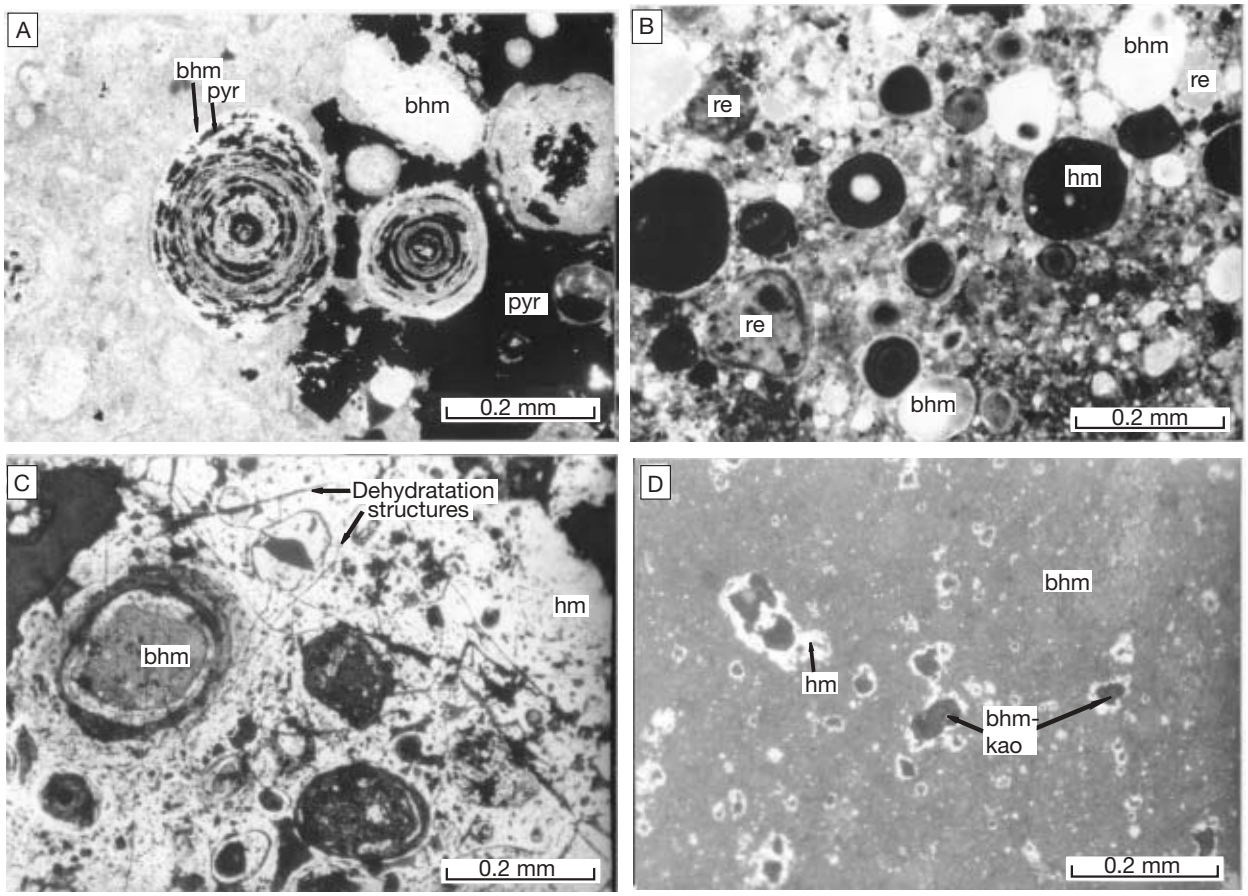

FIG. 6. Photomicrographs of ore types from the Doğankuzu bauxite deposit. A. Thin-section photomicrograph from the bottom sulfide section with ooids, from the fine-grained part of pisolitic ore, showing compositional banding; black area is pyrite (pyr) and white is böhmite (bhm); indicates pyritization of hematite. B. Thin-section photomicrograph of fine-grained part of pisolitic ore consisting of hematitic ooids (hm, black), böhmite ooids (white), and reworked bauxite fragments (re), indicating reworking or clastic accumulation. C. Polished-section photomicrograph showing böhmite-filled dehydadation structures and pseudo-oolitic texture developed in a hematite pisolite. D. Polished-section photomicrograph from massive ore showing scattered hematite ooids (white) in a fine-grained böhmite groundmass. kao = kaolinite. Polished-section photomicrographs used polarized light and oil immersion, and thin-section photomicrographs used polarized light.

after hematite, which exist in the pinkish-brown, low-grade bauxite. Sulfide-rich veins are composed of about 20 percent pyrite plus marcasite, with böhmite, diaspore, and minor anatase. Sulfides in vein-type deposits consist of idiomorphic and anhedral fine-grained pyrite with colloform böhmite. Microprobe studies of the sulfides indicate that the pyrite is nearly stoichiometric, with traces of Ti, Si, and Ca. Microbanding in the hematite and böhmite pisolites in the pisolitic-bauxite ores indicate fluctuating redox conditions during mineral precipitation.

Previous studies have not explained the common presence of sulfides in these deposits. Sulfides are not normally stable under oxidative or surface conditions. Özlü (1978) suggested that sulfides formed after bauxite was deposited. Textures such as pyrite pseudomorphs in the high-grade bauxites and compositionally banded ooids and pisolites with both sulfides and Fe oxides imply that sulfide minerals are diagenetic. The presence of sulfides indicates that the early diagenetic environment of the bauxite was reducing, at least at times.

Geochemistry of the Doğankuzu deposit

Geochemical data for 10 samples from the Doğankuzu bauxite ore were obtained by Özlü (1978) and are reproduced in Table 2. Averages of these analyses indicate that the ore consists of 61.1 percent Al_2O_3 associated with böhmite and diaspore, 17.4 percent Fe_2O_3 associated with hematite and minor goethite, 5.25 percent SiO_2 associated with kaolinite and minor smectite, and 2.9 percent TiO_2 associated with anatase. The large amount of Ti may have originated from alteration of a mica, such as biotite, or of clay minerals that were enriched in Ti. Alkali and alkali-earth elements are low in the bauxite, and total content is <1 percent. Average trace element concentrations of Zr (mean 533 ppm), V (mean 415 ppm), Cr (mean 369 ppm), Ni (mean 244 ppm), and Ga (mean 72 ppm) are three to four times their respective concentration in average shale (Krauskopf, 1982). These trace elements are commonly enriched in karst bauxites, and D'Argenio and Mindszenty (1995) called them bauxitophilic elements. The inter-element ratios among these trace elements

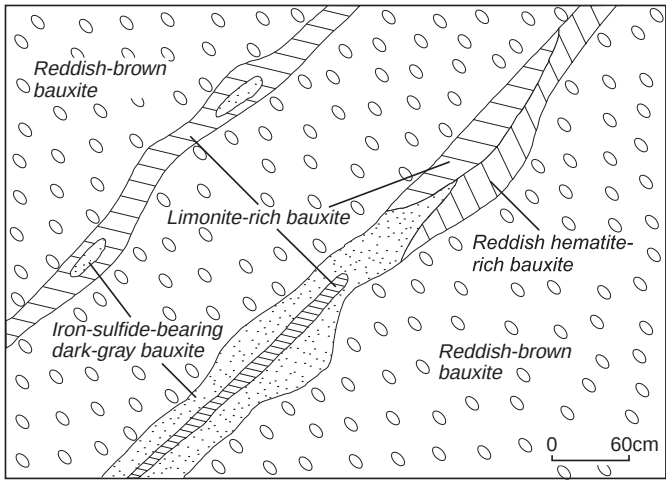

FIG. 7. Sketch of Fe sulfide-bearing bauxite vein in cross section, Doğankuzu bauxite deposit.

are virtually identical to those of mean continental shale (Krauskopf, 1982), indicating that the parent rock was likely typical continental aluminosilicate rock. It should be stressed that the average concentrations of Mn (27 ppm), Cu (<7.5 ppm), and Zn (<9 ppm) are very low and are respectively 1/32, 1/7, and 1/10 of their concentration in average shale.

Oxygen, carbon, and sulfur isotopes of the Doğankuzu deposit

Oxygen and carbon isotope compositions of host limestones vary within the narrow range of –2.5 to –5.2 per mil Peedee belemnite (PDB) and 0.3 to –4.8 per mil (PDB), respectively (Table 3). Stratigraphic variations are clearly seen in a $\delta^{18}O_{PDB}$ versus $\delta^{13}C_{PDB}$ plot and a plot of isotope compositions on a stratigraphic section (Figs. 9, 10). Limestones immediately underlying (footwall samples C-1 through C-5) and overlying (hanging-wall samples C-6 through C-11) the bauxite bed have comparable mean $\delta^{18}O_{PDB}$ compositions, –4.9 per mil and –4.8 per mil, respectively, but different mean $\delta^{13}C_{PDB}$ compositions, –4.2 per mil and –1.2 per mil. The limestone section (samples C-12 through C-15) stratigraphically overlying the hanging-wall limestone has a mean isotopic composition ($\delta^{18}O_{PDB}$ = –4.3‰ and $\delta^{13}C_{PDB}$ = –4.0‰) that is comparable to that of the footwall limestones (samples C-1 through C-5; Fig. 9). The stratigraphically highest limestone section sampled has the heaviest carbon and oxygen. Thus, the

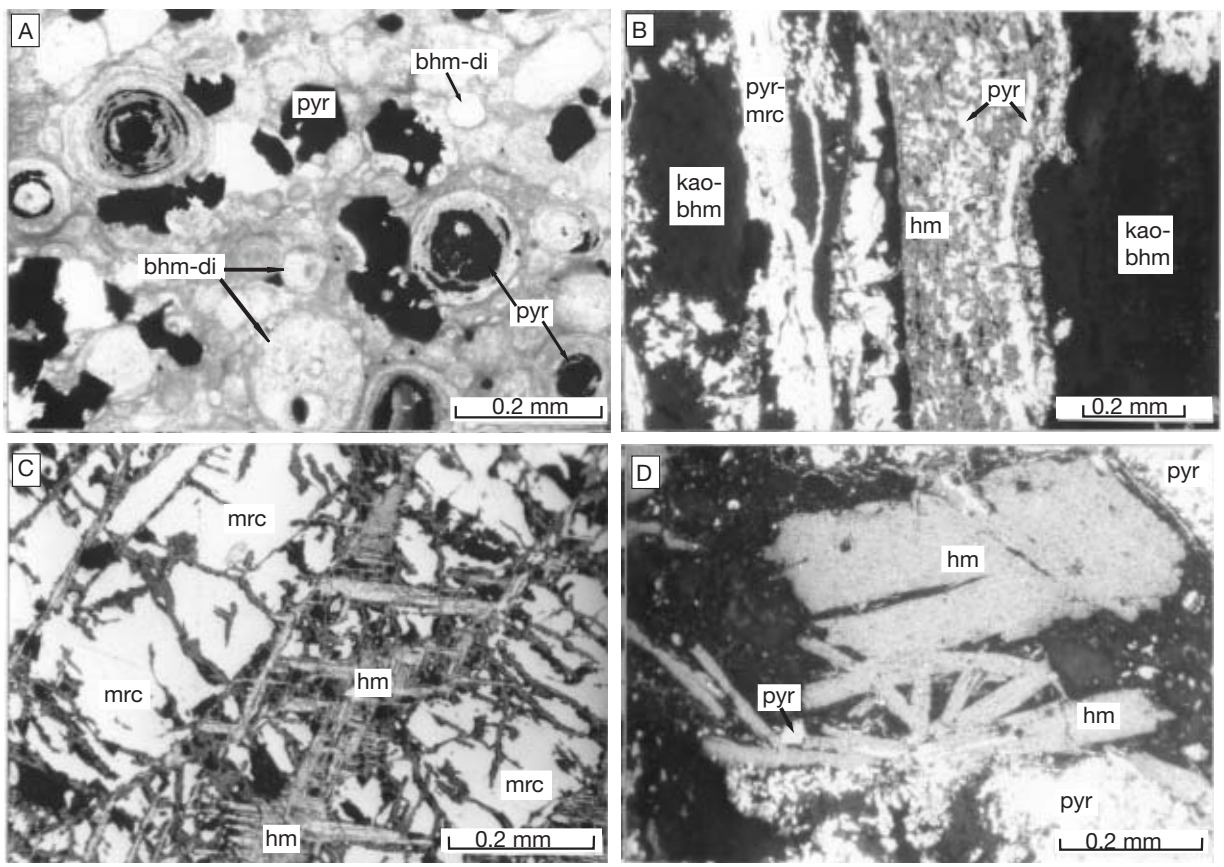

FIG. 8. Photomicrographs from the bottom sulfide zone of the Doğankuzu bauxite deposit. A. Thin-section photomicrograph of fine-grained part of oolitic ore showing böhmite (bhm)-diaspore (di) ooids (white) and pyrite (pyr, black). B. Polished-section photomicrograph of banding where pyrite plus marcasite (mrc, white) alternate with kaolinite (kao) and böhmite (black). hm = hematite. C. Polished-section photomicrograph showing alteration of marcasite (white) to hematite (gray) along crystallographic planes. D. Polished-section photomicrograph showing hematite laths (gray) within fine-grained pyrite. Polished section photomicrographs used polarized light and oil immersion, and thin-section photomicrographs used polarized light.

TABLE 2. Chemical Composition of Major Oxides (wt %) and Trace Elements (ppm) for 10 Massive and Oolitic Bauxite Ore Samples from the Doğankuzu Deposit (data from Özlü, 1978)

SiO_2	3.72	6.58	6.76	5.18	4.12	2.86	8.14	3.98	4.54	6.60
Al_2O_3	63.7	59.5	60.4	57.7	63.4	62.0	59.2	62.5	62.4	60.1
Fe_2O_3	16.3	18.0	16.3	21.0	16.3	19.2	16.4	17.0	16.5	17.4
TiO_2	2.91	3.04	2.58	2.80	2.82	2.83	2.92	3.30	3.17	2.97
CaO	0.11	0.28	0.14	0.17	0.22	0.25	0.14	0.06	0.08	0.03
MgO	0.12	0.12	0.32	0.34	0.16	0.14	0.20	0.16	0.24	0.30
Na_2O	0.26	0.21	0.49	0.27	0.17	0.19	0.06	0.05	0.08	0.06
K_2O	0.20	0.27	0.36	0.29	0.18	0.19	0.31	0.14	0.14	0.20
LOI	12.39	12.00	12.20	11.74	12.35	11.98	12.35	12.38	12.64	12.35
Total	99.71	100.00	99.55	99.49	99.82	99.64	99.72	99.57	99.79	100.01
Ga	78	70	70	62	77	71	70	75	76	74
Pb	80	86	83	76	83	91	89	82	88	75
Zn	<6	14	9	16	<6	9	13	<6	<6	<6
Zr	554	512	519	508	550	529	535	570	531	520
Cu	<6	<6	<6	9	<6	13	<6	11	<6	<6
Ni	220	226	233	209	205	210	383	236	235	283
Mn	20	31	35	37	30	34	22	15	16	26
Cr	377	319	480	284	328	213	532	341	399	416
V	415	409	429	385	387	478	330	396	400	522

isotopic composition of the limestone section has fluctuated several times during the interval measured. The nearly constant oxygen isotope composition of limestones immediately adjacent to the bauxite bed suggests that there was no significant change in climate during formation of those limestones, and thus climate change was likely not a factor in bauxite formation. The distribution of carbon isotope values indicate that productivity (terrestrial and/or marine) and burial of carbon may have been highest during deposition of the footwall limestone, decreased during deposition of the hanging-wall limestone, and then fluctuated after that. Oxidation of organic matter produced ^{12}C-rich CO_2 that was used to form the footwall limestone in conjunction with seawater bicarbonate.

TABLE 3. Carbon and Oxygen Isotopic Composition of Host-Rock Samples of the Doğankuzu Bauxite Deposit, Turkey

Sample	Rock type	$\delta^{13}C_{PDB}$	$\delta^{18}O_{PDB}$
Hanging-wall limestone			
C-19	Dolomitic limestone	–0.4	–4.0
C-18	Dolomitic limestone	–0.5	–2.5
C-17	Limestone	–0.1	–3.1
C-16	Dolomitic limestone	0.3	–2.9
C-15	Limestone	–3.8	–4.3
C-14	Limestone	–4.0	–4.5
C-13	Limestone	–4.8	–4.3
C-12	Limestone	–3.2	–4.1
C-11	Limestone	–1.1	–4.5
C-10	Limestone	–1.3	–4.5
C-9	Limestone	–0.7	–5.2
C-8	Limestone	–0.8	–5.2
C-7	Limestone	–1.4	–4.9
C-6	Limestone	–1.9	–4.5
Mean		–1.7	–4.2
Footwall limestone			
C-5	Limestone	–4.6	–4.8
C-4	Limestone	–4.4	–5.2
C-3	Limestone	–3.6	–5.0
C-2	Limestone	–4.1	–5.0
C-1	Limestone	–4.5	–4.7
Mean		–4.2	–4.9

The sulfur isotope compositions of Fe sulfides from the bottom sulfide zone of the bauxite bed (S-1 and S-2) and from the veins (S-3 and S-4) show a wide range, from 5.9 to –44.4 per mil (Table 4). The most negative values, obtained from samples S-2 and S-3, are typical of sulfides formed by bacterial-sulfate reduction, at temperatures <50°C, in euxinic environments where the rate of sulfate reduction was much slower that the rate of sulfate supply (Ohmoto and Rye, 1979). Sulfides formed under these conditions typically have $\delta^{34}S_{CDT}$ values of 40 to 60 per mil lower than those of the

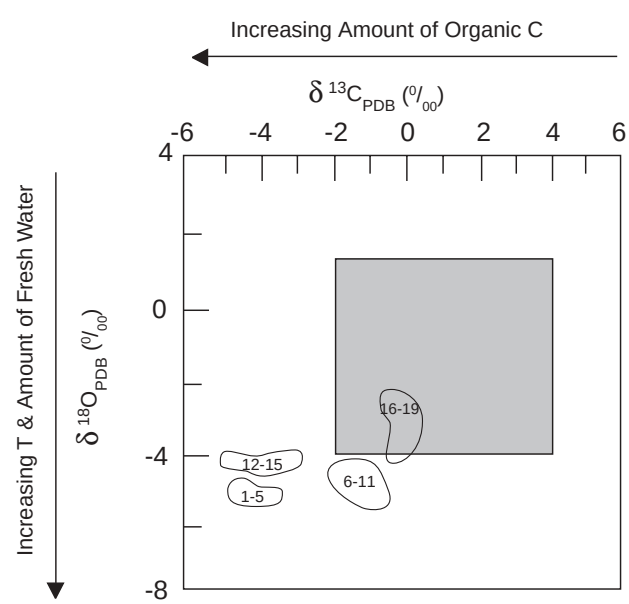

FIG. 9. Plot of $\delta^{18}O$ versus $\delta^{13}C$ showing fields that represent stratigraphic sections with similar isotope compositions. Circled numbers are limestone sample numbers: 1 to 5 = footwall limestone, 6 to 11 = hanging-wall limestone, and 12 to 15 and 16 to 19 = the next higher two stratigraphic intervals (see Figs. 4 and 10; samples are listed as C-1 through C-19 in Tables 1 and 3). The shaded square represents the isotopic field of shallow-water marine mollusks and foraminifera (Milliman, 1974).

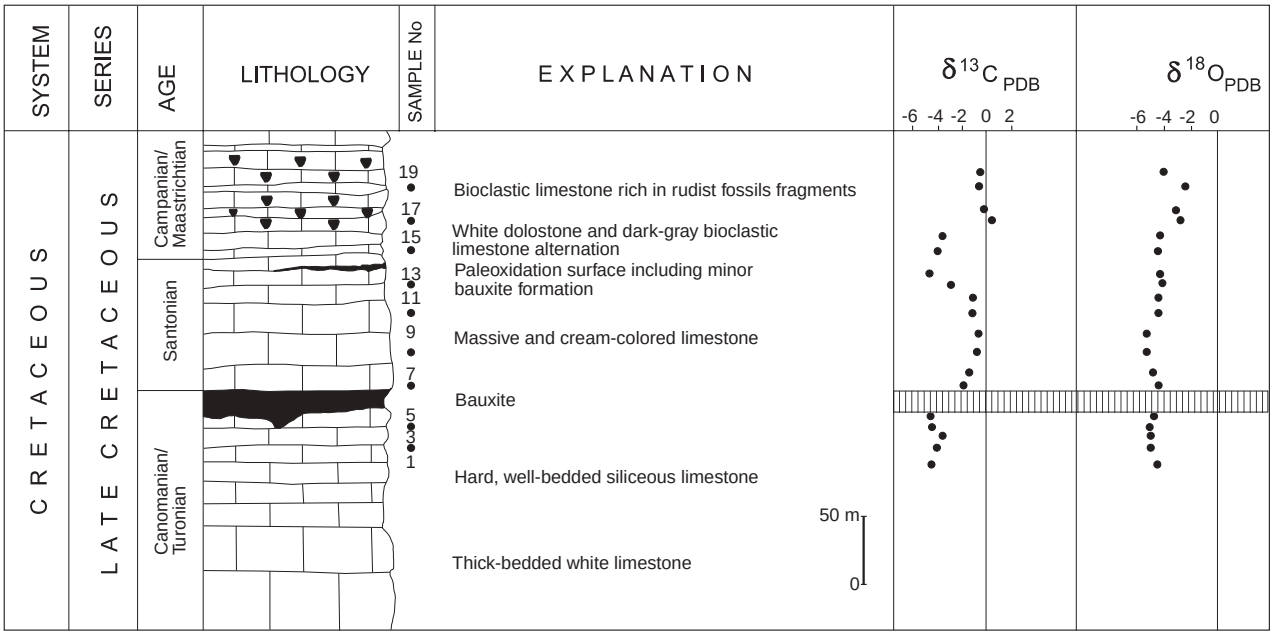

FIG. 10. Distribution of C and O isotopes with stratigraphic position and rock types at the Doğankuzu deposit; sample numbers are listed as C-1 through C-19 in Tables 1 and 3.

seawater sulfate that was reduced (ca. 15–20‰ during the Turonian; Strauss, 1997). The positive $\delta^{34}S_{CDT}$ values of samples S-1 and S-2 could have been produced in several ways, but they likely reflect Fe sulfide formed by bacterial reduction in shallow-marine or brackish-water environments where the rate of sulfate reduction was faster than the rate of sulfate supply (Ohmoto and Rye, 1979).

Discussion

The source of the Al, Fe, and Ti for the bauxite was the parent aluminosilicate host rock, which was most likely either an argillaceous sedimentary rock or a mica-rich granite and/or gneiss. Earlier workers emphasized that the Ordovician Seydişehir schist, consisting of metamorphosed shale and graywacke, was the most likely parent rock for the bauxites.

Abrupt accumulation of bauxitic material in depressions and sinkholes is indicated by intercalations of bauxite and calcareous conglomerate, reworked bauxitic material such as coarse and broken pisolites, and well-defined graded beds composed of flattened pisolites that occur as lenses in the bauxite. Mass-flow deposition of the bauxite is thought to have been triggered by tectonic activity because it accumulated predominantly in fault-bounded depressions and because of the abrupt (event-driven) nature of the deposition.

TABLE 4. Sulfur Isotope Composition of Pyrite from the Doğankuzu Bauxite Deposit, Turkey

Sample	S (wt %)	$\delta^{34}S_{CDT}$
S-1	9.03	5.9
S-1*	9.11	5.8
S-2	15.7	–44.1
S-3	18.8	–44.4
S-4	9.12	–7.8

*Duplicate analysis of separate aliquot

We propose that the bauxite formed in three stages. During stage 1, Al, Fe, and Ti were dissolved from the aluminosilicate parent rock under extremely acidic weathering conditions with pH < 4 (Fig. 11A). Under these conditions, Si would have remained in the intensely weathered deposit, whereas Fe, Al, and Ti would have been leached (e.g., Norton, 1973). The leached Fe, Al, and Ti were reprecipitated as simple oxides near the limestone surface where the acidic ground waters were neutralized (Fig. 11B). This process resulted in the accumulation of bauxitic materials, Fe and Ti oxides, and clay minerals on the limestone surface (bauxitic soil).

During stage 2, the bauxitic soils were transported a short distance to depressions and sinkholes in the limestone (Fig. 11C). Erosion of the bauxitic soil was promoted by rapid uplift caused by tectonic activity (see below), which produced the intercalation of calcareous conglomerate and bauxite by means of clastic deposition and mass movements. Thus, bauxitic soils were transported to fault-controlled basins and karst depressions, where they accumulated as relatively thick bauxite ores.

During stage 3, the ore was upgraded by in situ leaching and desilicification under conditions of a well-developed karst drainage system. Strata-bound sulfides also formed during stage 3, after deposition of the bauxite but prior to formation of the sulfide veins. Hematite-pyrite replacement relations show that redox conditions fluctuated several times during deposition and diagenesis of the strata-bound sulfides.

Textural and isotopic evidence suggests that formation of the three types of sulfides in the bauxites (bottom, top, and vein) took place during diagenesis (Fig. 12). Sulfides at the base of the bauxite bed formed earliest and likely precipitated after a marine transgression over the weathered surface and

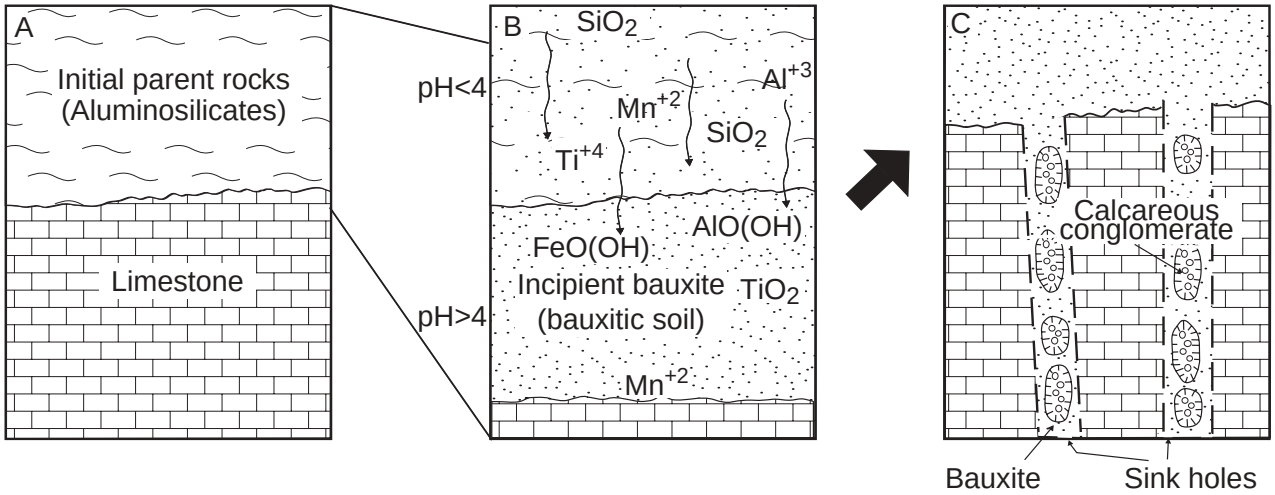

FIG. 11. Three-stage model for evolution of the bauxite deposits. A. Initial relationship of aluminosilicate parent rock to limestone. B. Stage 1 involved intense leaching of parent rock under low pH conditions that mobilized Al, Ti, Fe, and Mn, but not Si, and formed bauxitic soil, whereas Mn was transported out of the system under low Eh conditions. C. Stage 2 involved short transport of bauxitic soils to depressions and sinkholes in the limestone, where it was locally interbedded with calcareous conglomerate deposited by gravity mass-flow processes that may have been generated by tectonic activity. Stage 3 (not illustrated) involved upgrading of the bauxitic material through desilicification, and formation of sulfides (see Fig. 12).

the bauxite deposits (Fig. 12A). The early diagenetic environment in the bauxite was at times reducing, as indicated by pyrite formation after accumulation of the bauxite, diagenetic oxide-sulfide banding in pisolites and ooids, and formation of sulfide-rich horizons within the bauxite bed. Fluctuating redox conditions during early diagenesis are indicated by the occurrence of both pyrite replacement of hematite and hematite replacement of pyrite (at least three episodes are noted) and by the oxide-sulfide banding.

Iron in the bottom and top sulfides was derived from alteration of Fe hydroxide that accumulated with the bauxite. The source of the sulfur is thought to have been seawater sulfate, which was reduced to sulfide by bacterial processes, coupled with oxidation of organic matter (Fig. 12A, B) via a reaction such as

$$5Fe_2O_3 + 20SO_4^{2-} + 37.5CH_2O + 2.5H^+ \Rightarrow 10FeS_2 + 37.5HCO_3^- + 21.5H_2O \quad (1)$$

(e.g., Berner, 1970; Rickard, 1972; Goldhaber and Kaplan, 1974; Strauss, 1997). The bottom and top sulfide zones may represent horizons where a relatively persistent redox boundary had been established at different times as the result of the decay of organic matter, supply of Fe, and perhaps also establishment of a permeability barrier.

The sulfide veins formed last, along faults and fractures that crosscut and offset the strata-bound sulfide, most likely by two processes: precipitation (infilling) by the same process that formed the bottom and top sulfide zones and/or remobilization and subsequent reprecipitation of sulfides from the top or bottom sulfide zones entrained in fluids moving along the faults and fractures (Fig. 12C). The fault planes may have served as conduits for seawater once limestone had capped the bauxite. The lack of sulfide veins in both the underlying and overlying limestones indicates that Fe, which enriched only the bauxite, was the limiting element for sulfide formation.

Separation of metal oxides and passive margin metallogeny

Paleogeographic reconstruction of the Tethys Ocean in the region of the Taurides Mountains during the Santonian indicates that it was a passive-margin setting (Dercourt et al., 1985). The shallow-marine platform environment is thought to have been marked by fault-controlled depressions and highs (Fig. 13). Within this passive margin, the following conditions were required to fractionate the metal oxides that produced the various coeval ore deposits of southern Turkey. Aluminum and Ti were mobilized under low pH conditions associated with weathering of the parent rock that produced thick acidic soils. While Mn and Si were being transported to the ocean under low pH-Eh conditions, Fe was mostly trapped on land primarily as insoluble hydroxides along with Al hydroxides. In this way, Mn was fractionated from Al and Fe, and the Mn contributed to coeval, laterally adjacent, black shale-hosted Mn deposits offshore (Öztürk and Hein, 1997). The coeval Mn deposits likely accumulated in the oxygen-minimum zone of rapidly subsiding pull-apart basins associated with strike-slip faults (Maynard and Klein, 1995). This distribution of deposit types occurs throughout the Taurides and reflects the persistent geochemical conditions and paleoenvironments required for separation and accumulation of those metals. In fact, it is common to find that bauxite deposits throughout the entire Alpine region occur in a passive-margin sequence that coincided with Mn deposition in an adjacent relatively deep marine setting (Varnavas and Panagos, 1981; Öztürk and Hein, 1997). Our model for bauxite deposition and Mn, Fe, and Al fractionation (Fig. 13) shows that the separation of Fe and Mn occurred primarily on land, followed by transport of the Mn to the marine environment.

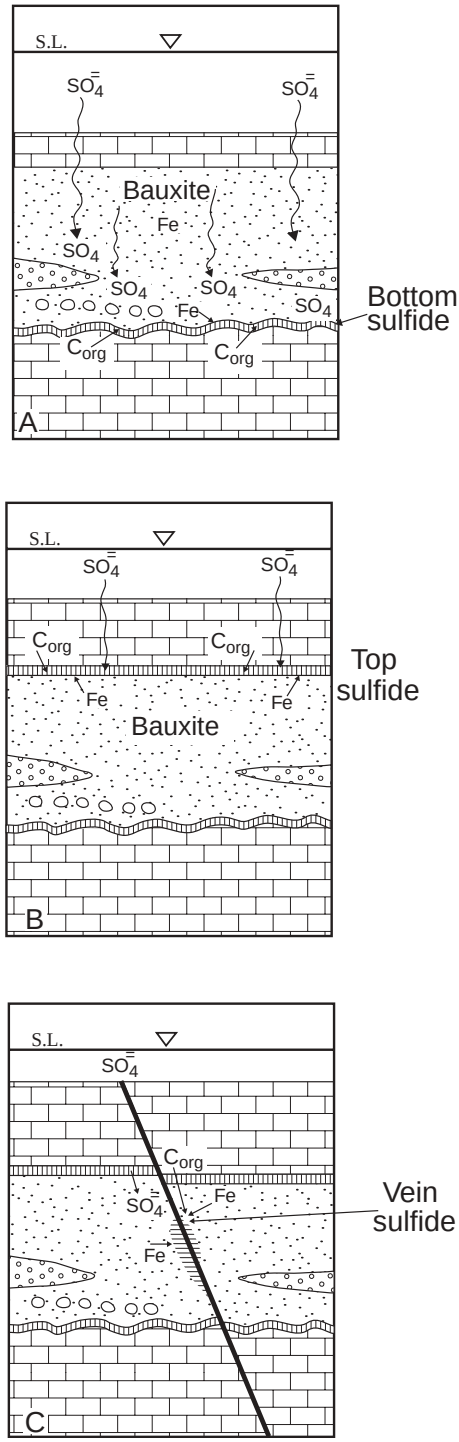

FIG. 12. Model for the evolution of bottom and top strata-bound sulfides and vein sulfide in the bauxite deposits during stage 3 diagenesis. A. Bottom sulfide zone formed by reduction of seawater sulfate and accompanied oxidation of organic matter during transgression of the sea and from Fe supplied by alteration of Fe hydroxides deposited with the bauxite. B. Top sulfide zone formed by the same geochemical processes as the bottom sulfides, but during somewhat later diagenesis; both zones likely represent locations of relatively persistent redox boundaries at different times. C. Sulfide vein crosscuts and offsets the two strata-bound sulfide layers and formed from the same geochemical process as the other sulfides, but after faulting fractured the rocks; sulfide from the top and/or bottom sulfide zones may have been partly remobilized and deposited along the faults and fractures.

Two mechanisms could have acidified the soil that formed from leaching of the parent rock during the Cenomanian and Santonian: acid rain associated with volcanic activity, which would have affected the land biota and ecology, or formation of thick soils and associated organic acids with development of extensive vegetation in a tropical climate. Volcanic material was not found in the stratigraphic succession that hosts the bauxite deposits and, therefore, we favor a dominantly climatic control on acidification of the soil. The carbon and sulfur isotope compositions emphasize the importance of organic matter and bacterial processes during deposition and mineralization, and they thus provide circumstantial evidence that organic acids may have been key in creating acidic environments and in mobilizing Al.

The regional (Alpine) paleoenvironments that promoted formation of the Mn and Al deposits likely reflected global geologic and oceanographic processes. Extensive oceanic volcanism and tectonism, high sea-level stands, and widespread oceanic anoxia characterized the Late Cretaceous Earth (Sinton and Duncan, 1997; Jones and Jenkyns, 2001). Deposition of Mn shifted from deep-sea environments to continental margin environments as demonstrated by formation of several large continental-margin Mn deposits at that time (Dickens and Owen, 1993), including those in the Taurides region. Globally extensive anoxia may also have contributed to the reducing conditions that allowed sulfides to form during transgression and early diagenesis.

Tectonic controls

Relatively rapid sea-level changes (transgressions and regressions) must have been related to tectonic activity because paleoclimates apparently did not vary much from prebauxite to postbauxite time on the basis of oxygen isotopes of the host limestones. A sea-level fall that exposed the limestone surface was likely the result of strike-slip faulting associated with closure of the ocean and local uplift of the passive margin. That uplift resulted in karstification and bauxite accumulation in depressions and sinkholes on the limestone surface. Subsequent transgression into the foreland basin that submerged the bauxite deposits resulted from shortening of the ocean basin and nappe emplacement, which took place from north to south in the region (Aubourg et al., 1997). That time was marked by bioclastic limestone deposition on the nappe ramp and by the overlapping of bauxite sediments by bioclastic limestones during the latest Cretaceous. Continental collision and uplift occurred at the end of the Eocene.

Acknowledgments

The authors wish to thank Kemal Erdogan for identifying the Cretaceous fossils, Cazibe Hosgören for drafting the figures, and Jennifer Dowling and Brandie McIntyre for technical help. J.B. Maynard, G. Bárdossy, S.P. Varnavas, C.N. Alpers, and M. Hannington provided excellent suggestions for improving this paper. Etibank Mining Company provided help during field studies.

January 25, 2001; February 21, 2002

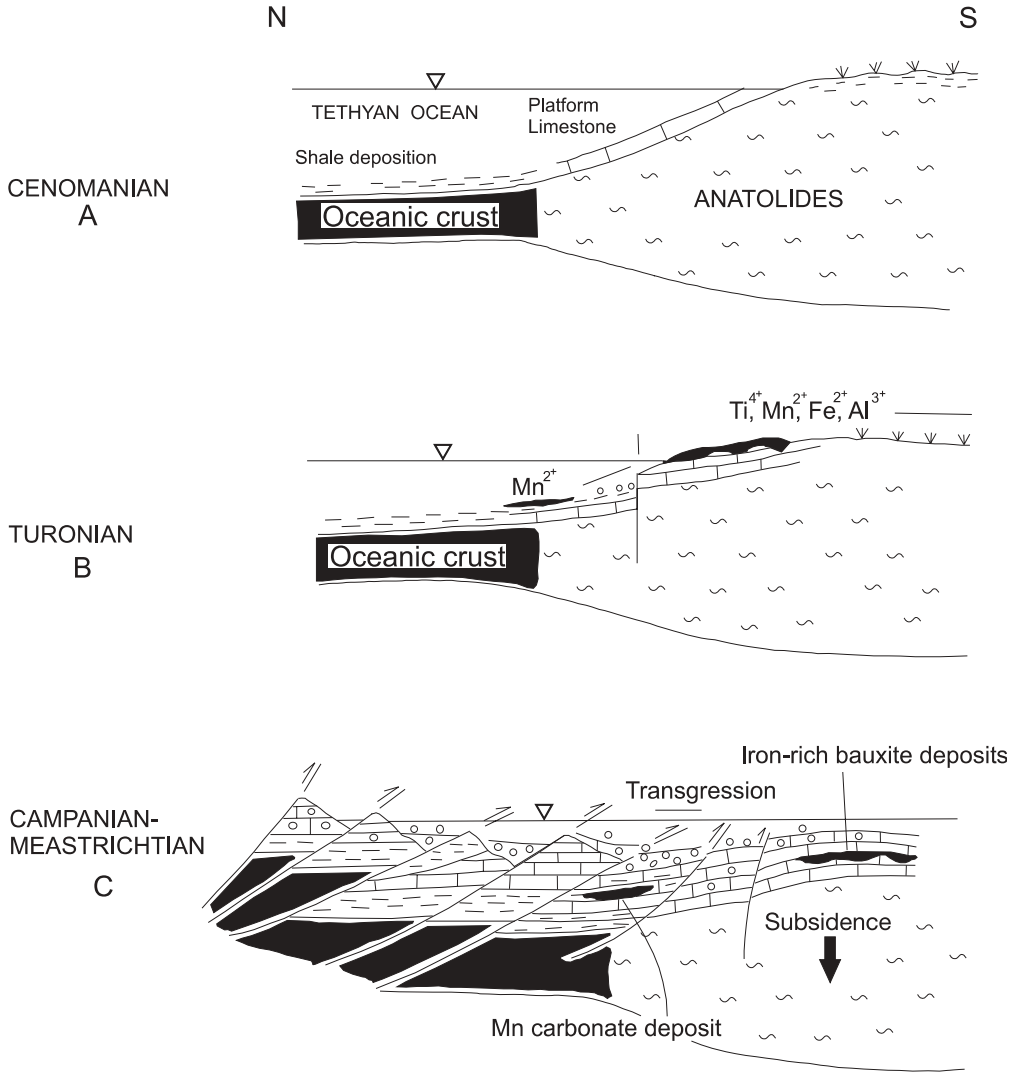

FIG. 13. Schematic cross section of the central Taurides showing a tectonic model for bauxite and Mn deposition during the Cretaceous, and fractionation of Al, Mn, and Fe associated with sea-level change on a passive continental margin. The triangles mark a tie point for the three diagrams. A. Platform limestone and shale deposition occurred at a passive margin of the Tethys Ocean from Early to Late Cretaceous. On land, extensive vegetation developed as the result of a humid climate and thereby created thick and acidic soils. Large amounts of organic matter were transported to the ocean, which is reflected in relatively ^{12}C-rich marine limestones (footwall rocks). B) Relative sea-level fall resulted from strike-slip faulting associated with closure of the ocean and local uplift of the passive margin. That uplift resulted in karstification and short transport of bauxitic soils formed from intensive leaching of aluminosilicate parent rock and accumulation in depressions and sinkholes. Aluminum, Fe, Mn, and Ti were mobilized on land and Al, Fe, and Ti hydroxides and oxides were deposited on the limestone surface owing to increased pH. Mn was transported to the ocean and deposited in muds as Mn carbonates (Öztürk and Hein, 1997). C) Transgression into the foreland basin resulted from shortening of the ocean basin and nappe emplacement. That time was marked by bioclastic limestone deposition on the nappe ramp and overlapping of bauxite sedimentation by bioclastic limestone deposition during latest Cretaceous.

REFERENCES

Atabey, M.E., 1976, Mineralogy, chemistry and origin of the Mortaş bauxite deposit, Seydişehir-Konya, Turkey: Bulletin of the Geological Society of Turkey, v. 19, p. 9–14.

Aubourg, C., Frizon de Lamotte, F., Posison, A., and Mercier, E., 1997, Magnetic fabrics and oblique ramp-related folding: A case study from the western Taurus (Turkey): Journal of Structural Geology, v. 19, p. 1111–1120.

Ayhan A., and Karadağ, M.M., 1985, Geology and origin of bauxitic iron and ferruginous bauxite deposits in the south of Şarkikaraağaç (Isparta): Bulletin of the Geological Society of Turkey, v. 28, p. 137–146.

Bárdossy, G., 1982, Karst Bauxites: Elsevier, Amsterdam, 441 p.

Bárdossy, G. and Combes, P.-J., 1999, Karst bauxites: Interfingering of deposition and palaeoweathering: International Association of Sedimentologists Special Publications, v. 27, p. 189–206.

Berner, R.A., 1970, Sedimentary pyrite formation: American Journal of Science, v. 268, p. 1–23.

Blumental, M., and Göksu, E., 1949, The geology and genesis of the bauxite occurrences of the Akseki region: Journal of Mineral Resources and Exploration Institute of Turkey, v. 14, p. 1–58.

Caillére, S., and Pobeguin, T., 1961, Sur les minéraux ferriféres dans une bauxites: Académe des Sciences (Paris): Comptes Rendus, v. 253, p. 288–290.

Çevrim, M., 1984, Die Zink-Blei-Vererzungen des Aladag-Gebietes/Türkei mit Betrachtungen zur Paläokarstentwicklung: Unpublished Ph.D. dissertation, Aachen, Germany, Aachen University, 184 p.

D'Argenio, B. and Mindszenty, A., 1995, Bauxites and related paleokarst: Tectonic and climatic event markers at regional unconformities: Eclogae Geologicae Helvetiae, v. 88, p. 453–499

Dercourt, J., Zonenshain, L.P., Ricou, L.E., Kazmin, V.G., Le Pichon, X., Knipper, A.L., Grandjacquet, C., Sborshchikov, I.M., Boulin, J., Sorokhtin, O., Geyssant, J., Lepvrier, C., Biju-Duval, B., Sbuet, J.C., Savostin, L.A., Westhpal, M., and Lauer, J.P., 1985, Presentation de 9 cartes paléogéographiques au 1:20,000,000 s'etendant de I'Atlantique au Pamir pour la periode du Lias a l'Actuel: Bulletin de la Societe Géologique de France, Huitieme Serie, v. 1, no. 5, p. 636–652.

Dickens, G.R., and Owen, R.M., 1993, Global change and manganese deposition at the Cenomanian-Turonian boundary: Marine Georesources and Geotechnology, v. 11, p. 27–43.

Franz, E.-Z., 1978, Synthetic solid solutions between goethite and diaspore: Mineralogical Magazine, v. 42, p. 159.

Glasby, G.P., 1997, Fractionation of manganese from iron in Archaean and Proterozoic sedimentary ores, *in* Nicholson, K, Hein, J. R., Bühn, B., and Dasgupta, S., eds., Manganese Mineralization: Geochemistry and Mineralogy of Terrestrial and Marine Deposits: Geological Society of London, Special Publication 119, p. 29–42.

Göksu, E., 1953, The geology, mineralogy and genesis of the bauxite deposits of the Akseki region: Bulletin of the Geological Society of Turkey, v. 4, p. 79–140.

Goldhaber, M.B. and Kaplan, I.R., 1974, The sulfur cycle, *in* Goldberg, E.D., ed., The Sea: v. 5, New York, Wiley, p. 569–655.

Güldalı, N., 1973, Seydişehir and Akseki bauxite deposits and their relation to paleokarst phenomena in Taurus Mountains, *in* Congress of Earth Sciences on the Occasion of the 50th Anniversary of Turkish Republic: Mineral Resources and Exploration Institute of Turkey Special Publication, p. 391–408.

Hem, J.D., 1972, Chemical factors that influence the availability of iron and manganese in aqueous systems: Geological Society of America Bulletin, v. 83, p. 443–450.

Hutchinson, C.S., 1983, Economic deposits and their tectonic setting: New York, Wiley, 365 p.

Jones, C.E., and Jenkyns, H.C., 2001, Seawater strontium isotopes, oceanic anoxic events, and seafloor hydrothermal activity in the Jurassic and Cretaceous: American Journal of Science, v. 301, p. 112–149.

Karadağ, M., 1987, The geological and petrographic and genetical investigation of the Seydişehir region bauxites: Unpublished Ph.D. dissertation, Selçuk, Turkey, Selçuk University, 265 p.

Krauskopf, K.B., 1982, Introduction to Geochemistry: New York, McGraw Hill, 617 p.

Maynard, J.B., and Klein, G.D., 1995, Tectonic subsidence analysis in the characterization of sedimentary ore deposits: Examples from the Witwaterstrand (Au), White Pine (Cu), and Molango (Mn): Economic Geology, v. 90, p. 37–50.

Milliman, J.D., 1974, Marine Carbonates: Berlin, Springer-Verlag, 375 p.

Monod O., 1977, Recherches géoloques dans le Taurus Ocidental au sud de Beyşehir (Turquie): Unpublished Ph.D. dissertation, France, Paris University, 442 p.

Norton, S.A., 1973, Laterite and bauxite formation: Economic Geology, v. 68, p. 353–361.

Ohmoto, H., and Rye, R.O., 1979, Isotopes of sulfur and carbon, *in* Barnes, H.L., ed., Geochemistry of Hydrothermal Ore Deposits: New York, Wiley, p. 509–567.

Ostwald, J., and Bolton, B.R., 1992, Glauconite Formation as a factor in sedimentary manganese deposit genesis: Economic Geology, v. 87, p. 1336–1344.

Özlü, N., 1978, Etude géologique minéralogue et géochmıque des bauxites de la région D'Akseki-Seydişehir Taurus occidental-Turquie: Unpublished Ph.D. dissertation, Pierre Marie Curie University, Paris, 455 p.

——1979, New facts on the genesis of the Akseki-Seydişehir bauxite deposits: Bulletin of the Geological Society of Turkey, v. 22, p. 215–226.

Öztürk, H., and Hein, J.R., 1997, Mineralogy and stable isotopes of black shale-hosted manganese ores, southwestern Taurides, Turkey: Economic Geology, v. 97, p. 433–444.

Öztürk, H., Hanilçi, N., and Işık, A., 1998, The geology and sulfide zones of the Doğankuzu and Mortaş bauxite deposits, Seydişehir, Turkey [abs.]: Geological Congress of Turkey, 52nd, Abstracts, p. 6.

Patterson, S.H., Kurtz, H.F., Olson J.C., and Neely, C.L., 1986, World Bauxite Resources: U.S. Geological Survey Professional Paper 1076-B, 151 p.

Rickard, D.T., 1972, Sedimentary iron sulfide formation: International Symposium on Acid Sulfate Soils, Wageningen, Proceedings, v. 1, p. 28–65.

Sawkins, F.J., 1984, Metal deposits in relation to plate tectonics: Berlin, Springer-Verlag, 325 p.

Sinton, C.W., and Duncan, R.A., 1997, Potential links between ocean plateau volcanism and global ocean anoxia at the Cenomanian-Turonian boundary: Economic Geology, v. 92, p. 836–842.

Strauss, H., 1997, The isotopic composition of sedimentary sulfur through time: Palaeogeography, Palaeoclimatology, Palaeoecology, v. 132, p. 97–118.

Tardy, Y., and Nahon, D., 1985, Geochemistry of laterites, stability of Al-goethite, Al-hematite, and Fe^{3+}-kaolinite in bauxites and ferricretes: An approach to the mechanism of concretion formation: American Journal of Science, v. 285, p. 865–903.

Valeton, I., Bierman, M., Reche, R., and Rosenberg, F.F., 1987, Genesis of nickel laterites and bauxites in Greece during the Jurassic and the Cretaceous and their relation to ultrabasic rocks: Ore Geology Reviews, v. 2, p. 359–404.

Varnavas, S.P., and Panagos, A.G., 1981, The genesis and preservation of fossil manganese nodules in the area of Panormo, Greece, *in* International Symposium on the Hellenic Arc and Trench, Athens, Proceedings, p. 390–408.

Wippern, J., 1962, The bauxites of the Taurides Region and their tectonic setting: Journal of Mineral Resources and Exploration Institute of Turkey, v. 58, p. 47–70.